2016-08-15

# Selecting optimum locations for co-located wave and wind energy farms. Part II: A case study

Astariz, S



10.1016/j.enconman.2016.05.078
Energy Conversion and Management

# Selecting optimum locations for co-located wave and wind energy farms. PART II: a case study

S. Astariz[a1], G. Iglesias[b]

[a] *University of Santiago de Compostela, EPS, Hydraulic Eng., Campus Univ. s/n, 27002 Lugo, Spain.*

[b] *University of Plymouth, School of Marine Science and Engineering, Drake Circus, Plymouth PL4 8AA, UK.*

## Abstract

Combined energy systems present an opportunity to enhance the competitiveness of renewables and overcome other challenges of these novel renewables by realising the synergies between them. Among the different possibilities for combined systems, this work focuses on wave and wind co-located farms with the aim of assessing their benefits relative to standalone wind farms. To this end we estimate the energy production, investigate the power smoothing and shadow effect, and quantify the reduction in downtime achieved by the co-located farm through a case study off the Danish coast – a promising area for co-located farms based on the available resource and other considerations including technical constraints. The analysis is carried out based on hindcast data and observations extending from 2005 to 2015, and by means of state-of-the-art numerical models of the wind and wave fields – WAsP and SWAN, respectively. It is found that the energy yield per unit area with the combined wave-wind farm increases by 3.4% relative to a standalone wind farm, the downtime periods decrease by 58% and the power output variability reduces by 12.5%. Moreover, the capital and operational expenditures (CAPEX and OPEX, respectively) would also be significantly reduced thanks to the synergies realised through the combination of wind and wave power.

[1] *Corresponding author*; email: sharay.astariz@usc.es; tel.: +34982823295; fax: +34982285926

**Keywords:** Wave energy; Wind energy; Co-located wind-wave farm; North Sea; Power smoothing; The shadow effect

**Nomenclature**

$AWT_k$: percentage of Accesible Wind Turbines during $k$ % of time

$b$: spacing between the piles of the wind turbines (m)

$c$ ($\tau$): cross-correlation factor between two variables for a time lag $\tau$

$c_t$: transmission coefficient of the offshore wind turbines

$c_x$: spatial velocities in the $x$ components ($ms^{-1}$)

$c_y$: spatial velocities in the $y$ components ($ms^{-1}$)

$c_\theta$: rate of change of group velocity which describes the directional ($\theta$) rate of turning due to changes in currents and water depth

$c_\sigma$: rate of change of group velocity which describes the frequency ($\sigma$) shifting due to changes in currents and water depth

$C_d$: drag coefficient of the wind turbine piles

$d$: water depth (m)

$D$: rotor diameter (m)

$D_p$: diameter of the wind turbine piles (m)

$E$: energy density ($Jm^{-3}$)

EMODnet: European Marine Observation and Data Network

ERDF: European Regional and Development Fund

$f$ : wave frequency ($s^{-1}$)

$g$: gravity acceleration ($ms^{-2}$)

$H$: height at which the wind speed is measured (m)

$H_{m0}$: significant wave height (m)

$\bar{H}_{m0}$: average significant wave height (m)

$H_{m0,max}$: maximum value of the significant wave height (m)

$H_s$: significant wave height (m)

$(H_{s,b})_i$: significant height incident on the *i*-th wind turbine in the baseline scenario, i.e. without WECs (m)

$(H_{s,W})_i$: significant height incident on the *i*-th wind turbine with co-located WECs (m)

$HRC_j$: significant wave height reduction along the *j*-th row of wind turbines. This non-dimensional index reflects the wave recovery with increasing distance from the WECs

*HRF*: wave Height Reduction within the Farm. It is a non-dimensional parameter that provides information about the average wave height reduction within the wind farm

*IA*: increase in the accessible timeframe for O&M achieved with co-located WECs

$J$: raw wave power ($kWm^{-1}$)

$\overline{J}$: average raw wave power ($kWm^{-1}$)

$\overline{J}_{farm}$: time-averaged power generated by the WECs (kW)

$J_{W,i}$ : is the power generated by the *i*-th WEC (kW)

*k*: percentage of time during which the wind turbines are accessible

*L:* distance between the twin bows of a single WaveCat WEC (m)

*m*: number of turbines in the *j*-th row

$m_{n:}$ spectral moment of order *n*

$n_T$ : total number of time points

$n_W$: total number of WECs or wind turbines

*N:* wave action density spectrum (Js)

O&M: Operation & Maintenance

$P$: raw wind power ($kWm^{-2}$)

$\overline{P}$: average raw wind power ($kWm^{-2}$)

$\overline{P}_{farm}$: time-averaged power generated by the wind turbines (kW)

$\bar{P}_{W,i}$: is the power generated by the *i*-th wind turbine (kW)

PDA: Peripherally Distributed Array

$R^2$: coefficient of determination

RES: Renewable Energy Directive (2009/29/EC)

*RMSE*: Root Main Square Error $S_{tot}$: the energy density source terms which describe local changes to the wave spectrum ($Js^{-1}$)

SWAN: Simulating WAves Nearshore

*t*: a point in time (s)

*T*: total number of time points considered (s)

$T_b$: total number of hours per year with Hs ≤ 1.5m for the baseline scenario, i.e. isolated turbines (h)

$T_e$: energy period (s)

$\bar{T}_e$: average energy period (s)

$T_{e,max}$: maximum energy period (s)

$T_{mo1}$: mean wave period (s)

$T_W$: total number of hours per year when $H_s$ within the wind farm is lower or equal to 1.5 m with co-located WECs

*THD*: Total Harmonic Distortion

$U_w$: wind speed ($ms^{-1}$)

$U_{10m}$: wind speed at 10 m above the sea level ($ms^{-1}$)

$\bar{U}_{10m}$: average wind speed 10 m above the sea level ($ms^{-1}$)

$\bar{U}_{10m,max}$: maximum value of the wind speed 10 m above the sea level ($ms^{-1}$)

WAsP: Wind Atlas Analysis and Application Program

WEC: Wave Energy Converter

*z*: roughness length (m)

$\rho_a$: air density (kgm$^{-3}$)

$\rho_w$: sea water density (kgm$^{-3}$)

$\theta$: propagation direction ($^o$)

$\sigma$: standard deviation

$\mu$: average value

## 1. Introduction

The Renewable Energy (RES) Directive (2009/29/EC) established an EU target of a 20% share of renewable energy in the total energy consumption by 2020. Recently, at the Paris climate conference (COP21) in December 2015, 195 countries adopted the first-ever universal, legally binding global climate deal. The agreement set out a global action plan to put the world on track to avoid dangerous climate change by limiting global warming to well below 2°C. The agreement is due to enter into force in 2020. In this context, marine energy [1] emerges as one of the most promising alternatives to fossil fuels due to its substantial potential for electricity production [2], not least through the combination of various renewables in the same marine space [3], which can significantly enhance marine energy competitiveness [4]. Co-located projects are a solution to simultaneously tackle two major challenges: reducing technology costs [5] and achieving a more sustainable use of natural resources [6]. In particular, this research deals with the co-location of Wave Energy Conversion (WEC) technologies into a conventional offshore wind farm [7]. The addition of co-located Wave Energy Converters (WECs) to wind farms [8] is supported by a number of synergies ranging from an increase in the energy yield [9] to a reduction in the operation and maintenance cost [10] and smoothed power output [11].

In Part I of this work, the wave resource off the Danish coast was characterised in order to determine the best location for a co-located wave and wind energy farm. The aim of Part II is to define a co-located wave and wind farm at this location and assess its benefits relative to a standalone, conventional offshore wind farm. The co-located farm is designed on the basis of the current offshore farms characteristics and the results of previous studies concerning the most convenient co-located farm layout [12]. Hourly wave and wind observations from 2005 to 2015 combined with hindcast data are implemented on two numerical models: WAsP (Wind Atlas Analysis and Application Program) and SWAN (Simulating WAves Nearshore). The former is an industry-standard software for predicting the wind climate, wind resource, and power production from wind farms; and the latter is a third-generation numerical model that calculates wave generation and propagation.

The differences between the combined system and the conventional wind farm are quantified in terms not only of the global power production but also the performance of the devices, the downtime periods and the power variability. Moreover, the enlarged weather windows for O&M (Operation and Maintenance) thanks to the shadow effect of the co-located WECs are determined.

## 2. Materials and Methods

### 2.1. Wave and wind numerical models

The wind resource assessment and wind farm calculations were carried out by means of the WAsP (Wind Atlas Analysis and Application Program) software [13], which is an implementation of the so-called wind atlas methodology [14]. The program employs a comprehensive list of models for projection of the horizontal and vertical extrapolation of wind climate statistics [15]. It is a linear numerical model based on the physical

principles of flows in the atmospheric boundary layer, capable of describing wind flow over different terrains, close to sheltering obstacles and at specific points. Moreover, WAsP models the estimated power loss in wind farms due to the wind speed reduction in wakes from up-wind turbines [16]. In terms of wind farm modelling, the wake model in the commercial version is based on Katic et al. [17], using a linear expansion of the wake diameter set with a wake decay coefficient − a value of 0.04 or 0.05 is recommended for offshore applications [18].The model has been amply validated through a number of comparisons between measured and modelled wind statistics and wind farm production [19].

The available wave resource was assessed through the third-generation numerical wave model SWAN (Simulating WAves Nearshore). This model was successfully applied to examining the impact of wave farms on the wave conditions in their lee in recent studies such as [20] or [21]. It computes the evolution of random waves accounting for refraction, wave generation due to wind, dissipation and non-linear wave-wave interactions [22]. The evolution of the wave field is described by the action balance equation,

$$\frac{\partial}{\partial t} N + \frac{\partial}{\partial x} c_x N + \frac{\partial}{\partial y} c_y N + \frac{\partial}{\partial \sigma} c_\sigma N \frac{\partial}{\partial \theta} c_\theta N = \frac{S_{tot}}{\sigma} , \quad (1)$$

where $t$ is time (s), $c_x$ and $c_y$ are spatial velocities in the $x$ and $y$ components ($ms^{-1}$), $c_\theta$ and $c_\sigma$ are rates of change of group velocity which describe respectively the directional ($\theta$) rate of turning and frequency ($\sigma$) shifting due to changes in currents and water depth, $N$ is wave action density, and $S_{tot}$ are the energy density source terms which describe local changes to the wave spectrum. The model was implemented on a computational grid encompassing an area of approx. 134 km × 167 km with a resolution of 300 m × 300, and a nested grid focused on the co-located farm location covering an area of 8.5

km × 8.5 km with a resolution of 17 m × 17 m. Bathymetric data from the European Marine Observation and Data Network (EMODnet) were interpolated onto this grid. The wind turbines and WECs were implemented on SWAN as individual obstacles characterised by a transmission coefficient [23]. For wind turbines the transmission coefficient, $C_t$, was computed from

$$C_t = 4\left(\frac{d}{H_s}\right) E\left[-E + \sqrt{E^2 + \frac{H_s}{2d}}\right] , \quad (2)$$

$$E = \frac{C_d\left(\frac{b}{D_p+b}\right)}{\sqrt{1-\left(\frac{b}{D_p+b}\right)^2}}, \quad (3)$$

where $d$ is water depth (m), $H_s$ is incident significant wave height (m), $D_p$ is the pile diameter (m), $b$ is the pile spacing (m), and $C_d$ is the drag coefficient. For a smooth pile, as in this case, $C_d$ is equal to 1 [24]. For WECs, the transmission coefficient values were obtained from laboratory tests reported in [25].

### 2.2. Indicators

The available wind power ($P$) is given by

$$P = \frac{1}{2}\rho_a U_w^3 , \quad (4)$$

where $U_w$ is the wind speed, and $\rho_a$ is the air density, assumed equal to 1.23 kg/m$^3$, considering an average air temperature of 5 °C [26]. Wind speeds are often available from meteorological observations measured at a height of 10 m. However, hub heights of offshore wind turbines are usually 40 to 80 m [27]. The following equation allows the conversion of wind speed values measured at a certain height to the corresponding values at the hub height (or any other height of interest) [28]:

$$U_{w1} = U_{w2} \frac{\ln (H_1/z)}{\ln (H_2/z)}\,, \tag{5}$$

where $U_{w1}$ is the wind speed to be calculated at the height $H_1$, $U_{w2}$ is the measured wind speed at the height $H_2$, and $z$ is the roughness length.

The available wave power ($J$) can be computed from [29]:

$$J = \frac{\rho_w g^2}{64\pi} H_{mo}^2 T_e\,, \tag{6}$$

where $\rho_w$ is the sea water density (1027 kg/m$^3$, considering an average water salinity concentration of 33 ppm and an average water temperature of 7 °C), $g$ is the gravitational acceleration ($g$ = 9.82 m/s$^2$), $H_{m0}$ is the significant wave height, and $T_e$ is the energy period, which is defined in terms of spectral moments as follows:

$$T_e = \frac{m_{-1}}{m_0}, \tag{7}$$

where $m_n$ represents the spectral moment of order $n$, which is given by:

$$m_n = \int_0^{2\pi} \int_0^{\infty} f^n E(f,\theta) df d\theta\,, \tag{8}$$

where $f$ is the wave frequency and $E = E(f, \theta)$ is the energy density with $\theta$ the propagation direction. The energy period can be estimated as $T_e$ = 1.14 $T_{mo1}$ [1].

The power variability was analysed through statistical indicators such as the standard deviation ($\sigma$) or confidence intervals [30]. The variability is important as the peak-to-average ratio has been identified as a major cost driver in renewable energy systems [31]. Moreover, for co-located wave and wind farms the analysis of the wave-wind correlation is fundamental. It was quantified by means of the cross-correlation factor, $c(\tau)$,

$$c(\tau) = \frac{1}{T} \sum_{j=1}^{n_T-\tau} \frac{[x(k)-\mu_x][y(k-\tau)-\mu_y]}{\sigma_x \sigma_y}\,, \tag{9}$$

where $\mu_x$, $\mu_y$ and $\sigma_x$, $\sigma_y$ are the mean and standard deviation of two generic signals *x* and *y*, and $\tau$ is the time lag.

The time-averaged power generated by the WECs and wind turbines, $\bar{J}_{farm}$ and $\bar{P}_{farm}$ respectively, was calculated as:

$$\bar{X}_{farm} = \frac{1}{T} \sum_{i=1}^{n_W} \sum_{j=1}^{n_T} (\overline{X}_{W,i})_t \,, \tag{10}$$

where $\bar{X}$ can stand for wave or wind power production, the index *i* designates a generic WEC or wind turbine, $n_W$ is the total number of WECs or wind turbines, *j* represents a point in time, $n_T$ is the total number of time points considered and $\overline{X}_{W,i}$ is the power generated by the *i*-th WEC or wind turbine. It is assumed that the devices are operating 95% of the time in a typical year [32].

The power smoothing – resulting from aggregating power from diverse resources [33] – was assessed through the Total Harmonic Distortion (*THD*), which can be defined as

$$THD = \frac{\sigma}{\bar{x}}, \tag{11}$$

where $\bar{x}$ is the average power output and can refer to wave power (*J*), wind power (*P*) or wave and wind power (*J*+*P*).

Harsh sea conditions could increase downtime due to delays to maintenance and repairs. In the case of wind farms, the operational limit to workboats is a significant wave height of 1.5 m [34]. Co-located WECs, extracting energy from the incoming waves, provide a less energetic wave climate within the farm and thereby increase the duration and number of the weather windows to carry out maintenance; this is known as the shadow effect [10, 35, 36]. To quantify the shadow effect of the co-located WECs the significant wave Height Reduction within the Farm (*HRF*) (Eq. 12) and the significant wave Height Reduction along the *j*-th Column of wind turbines ($HRC_j$) (Eq. 13) indices

were defined. They provide, respectively, information about the average wave height reduction and the wave recovery with increasing distance from the WECs.

$$HRF\ (\%) = \frac{100}{n}\sum_{i=1}^{n_W}\frac{1}{(H_{s,b})_i}\left[(H_{s,b})_i - \ (H_{s,W})_i\right], \tag{12}$$

where the index *i* designates a generic turbine of the wind farm, $n_W$ is the total number of turbines, $(H_{s,b})_i$ is the significant height incident on the *i*-th turbine in the baseline scenario (without WECs), and $(H_{s,W})_i$ is the significant height incident on the *i*-th turbine with co-located WECs.

$$HRC_j(\%) = \frac{100}{m}\sum_{i=1}^{m}\frac{1}{(H_{s,b})_i}\left[(H_{s,b})_i - \ (H_{s,W})_i\right], \tag{13}$$

where the index *i* denotes a generic turbine of the *j*-th row (row of wind turbines numbered from the north to the south) of the wind farm, and *m* is the number of turbines in the *j*-th row.

The Increased Accessibility (*IA*) (Eq. 14) is a nondimensional index quantifying the increase in the timeframe accessibility to the wind turbines – percentage of time when the significant wave height is lower than 1.5 m in the vicinity of the wind turbines – thanks to the co-located WECs:

$$IA\ (\%) = \frac{T_W - T_b}{T_b} \times 100\ , \tag{14}$$

where $T_W$ and $T_b$ are the total number of hours per year when $H_s$ within the wind farm is below or equal to 1.5 m with co-located WECs and in the baseline scenario, respectively.

Finally, the index $AWT_k$ (Eq. 15) quantifies the percentage of wind turbines that are accessible during *k*% of the time:

$$AWT_k = \frac{Accesible\ wind\ turbines}{Total\ number\ of\ wind\ turbines} \times 100\ , \tag{15}$$

where *k* is the percentage of time during which the wind turbines are accessible. In this study this parameter was assessed for *k* = 100%, 90%, 80%, 70% and 60%.

### 2.3. Study area

Previous studies have identified the North Sea as one of the best areas for deploying co-located farms due to the available resource and the moderate water depths [37, 38]. The present study focuses on the northwest Danish coast, which offers plenty of opportunity for marine energy [39].


Figure 1. The Northwest Danish coast (the red framed area).

Based on the analysis of hourly series of wave and wind data from 2005 to 2015, the site of coordinates (56.65ºN, 8.03ºE) was identified as the best location for deploying a co-located farm in terms of wave and wind power, power variability, correlation between waves and winds, distance from shore and water depth. Hindcast data from WaveWatch III, a third-generation offshore wave model, were used in conjunction with metocean data from February 2005 to January 2015 kindly provided by the Horns Rev wind farm.

The wave climate at this site is characterised by an average significant wave height of 1.5 m (Table 1) and 315º as predominant wave direction (Figure 2). The Jutland Peninsula shelters the area from southeasterly waves so the potential decreases clearly from this direction. The analysis of the wind direction (Figure 3) is also important in planning the wind farm layout. The predominant wind directions are from the III and IV quadrants, with significant westerly components. The mean wind speed was 8.7 m/s (Table 1).

Table 1. Most relevant wave and wind statistics of the site point no. 43. $\overline{H}_{mo}$: average significant wave height, $H_{m0,max}$: maximum value of the significant wave height, $\overline{T}_e$: average energy period, $T_{e,max}$: maximum energy period; $\overline{U}_{10m}$: average wind speed at 10 m above the sea level, $U_{10m,max}$: maximum wind speed at 10 m above the sea level.

| | | |
|---|---|---|
| Wave | $\overline{H}_{mo} \pm \sigma$ (m) | 1.53 ± 1.12 |
| | $H_{m0,max}$ (m) | 9.66 |
| | $\overline{T}_e$ (s) | 5.86 |
| | $T_{e,max}$ (s) | 18.55 |
| Wind | $\overline{U}_{10m} \pm \sigma$ (m s$^{-1}$) | 8.67 ± 3.76 |
| | $U_{10m,max}$ (m s$^{-1}$) | 28.94 |

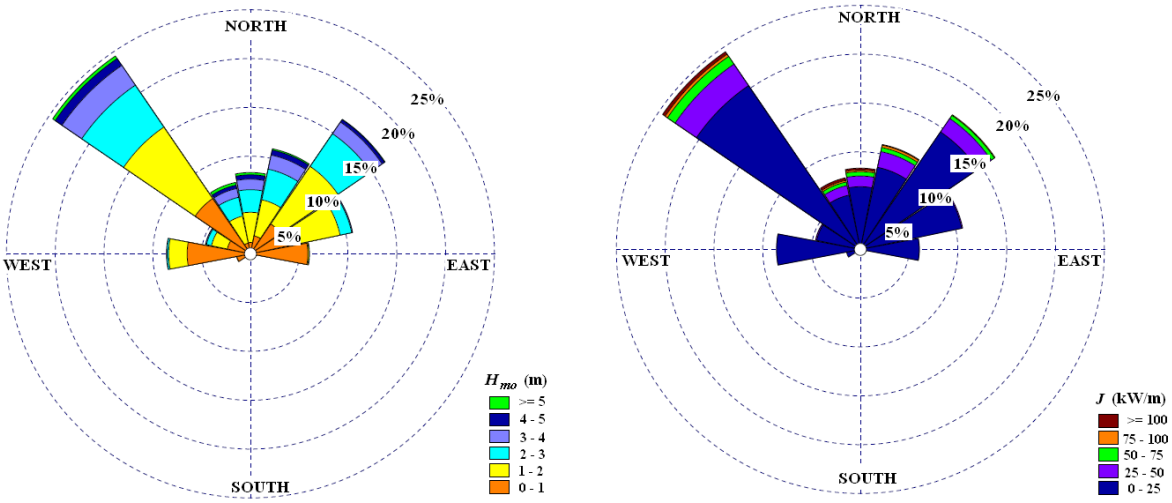


Figure 2. Wave rose (left) and wave power rose (right) for site no. 43 for the total study period (from February 2005 to January 2015)

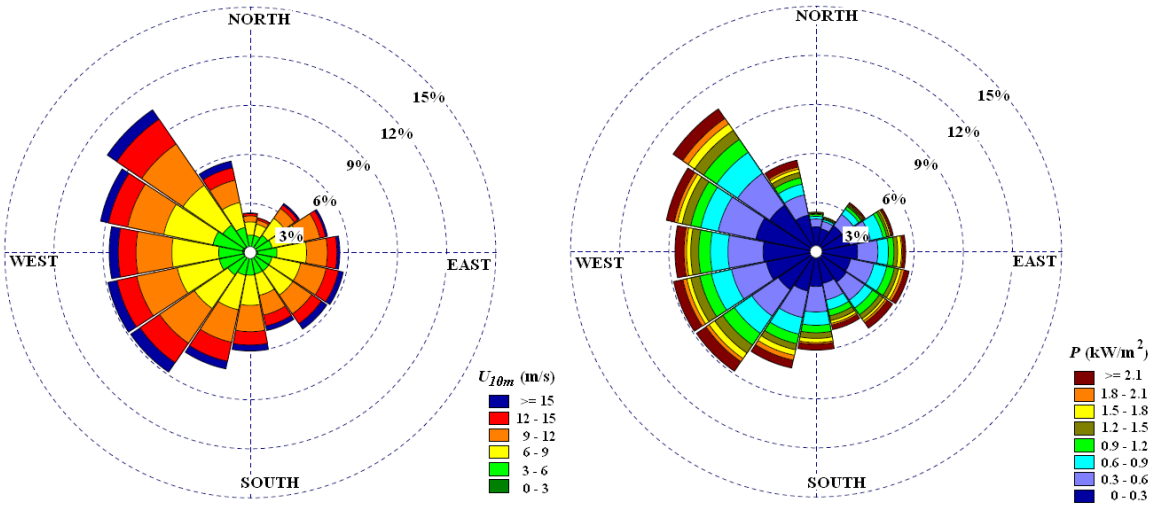


Figure 3. Wind rose (left) and wind power rose (right) for site no. 43 for the total study period (from February 2005 to January 2015.

### 2.3. Co-located wave and wind farm layout

At present the average offshore wind farm off the Danish cost is composed by 37 wind turbines with an installed capacity of 98 MW [40]. However, the current tendency is towards larger farms, composed by more than 80 turbines, and with larger turbines. The average turbine size is expected to be around 5 MW in the years to come [41].

The selection of the substructure is directly dependent on the water depth [8], which was around 20 m in this case. Monopile is the most cost-effective substructure type for offshore wind energy conversion systems due to its simple global design. In practice it is feasible for water depths of up to 35 m; in deeper water other substructures are employed, e.g. jacket frames or tripods [8].

As for the wind farm layout, many studies have been carried out by different researchers with a view to its optimization [42]. In spite of recommendations that wind turbines should not be installed in grids but instead scattered throughout the farm [43-45], currently wind farms are commonly ordered in rows perpendicular to the prevailing

wind direction [46] or staggered for the main wind direction to maximise the energy output [47]. Indeed, [47] stated that 10% extra power output can be captured from the staggered wind farm. For this reason, a staggered wind farm was proposed in this work. As for the geometry of the park, existing large wind farms have adopted square arrangements balancing energy output and cabling costs [48]. The location of the turbines is often optimized in order to minimize the wake effect – the shading effect of a wind turbine on other wind turbines downstream from it [49]. Using greater spacing between turbines implies less interaction but increased costs for array cables [50, 51]. In this sense, there exist discrepancies in the literature about the most convenient distance between turbines. For instance, it has been stated [52] that the distance between turbines in a row is usually of the order of 5–10 rotor diameters (5*D*–10*D*,where *D* is the rotor diameter), while other studies [53-55] considered that 7*D*–12*D* is typically the distance between rows.

Accounting for all these factors, the proposed farm in this study was composed by 80 turbines, erected on a grid of 8 rows with monopiles as substructures. The distance between the individual turbines and rows was 8*D* – average value in the literature, i.e. 960 m. The farm layout was staggered with respect to a westerly wind to maximise the energy output, and covered an area of 58 $km^2$ with a density of 5 $MW/km^2$.

A comparison between the Siemens Wind Turbine SWT-3.6-120 [56] and other larger turbines, such as the REpower 5M [57], AREVA M5000 turbine [58] or NREL 5-MW [59], was carried out to select the wind turbine according to the site characteristics. These turbines have similar values of cut-in, rated and cut-out wind speeds but different rotor diameters and rated power values (Table 2). However, analysing their power curves and the existing wind resource it was found that they would be operating over

50% of their capacity during 70% and 60% of the time in the case of the SWT-3.6-120 and 5MW turbines, respectively. Moreover, SWT-3.6-120 would require monopiles with a smaller diameter due to the lower weight of the turbine, which would reduce the foundation cost. For these reasons, the Siemens Wind Turbine SWT-3.6-120 was selected.

Table 2. Technical characteristics of the Siemens Wind Turbine SWT-3.6-120, REpower 5M, AREVA M5000 and NREL 5-MW turbines.

| | | | | | |
|---|---|---|---|---|---|
| SWT-3.6-120 | Nominal power | 3.6 MW | REpower 5M | Nominal power | 5 MW |
| | Rotor diameter | 120 m | | Rotor diameter | 126 m |
| | Hub height | 90 m | | Hub height | 90 -120 m |
| | Cut-in wind speed | 3-5 m/s | | Cut-in wind speed | 3.5 m/s |
| | Rated wind power | 12-13 m/s | | Rated wind power | 13 m/s |
| | Cut-out wind speed | 25 m/s | | Cut-out wind speed | 30 m/s |
| Areva M5000 | Nominal power | 5 MW | NREL 5-MW | Nominal power | 5 MW |
| | Rotor diameter | 135 m | | Rotor diameter | 126 m |
| | Hub height | 70 -90 m | | Hub height | 90 m |
| | Cut-in wind speed | 4 m/s | | Cut-in wind speed | 3 m/s |
| | Rated wind power | 12.5 m/s | | Rated wind power | 11.4 m/s |
| | Cut-out wind speed | 25 m/s | | Cut-out wind speed | 25 m/s |

As for the co-located WECs, the WaveCat was selected [60]: a floating offshore WEC whose principle of operation is wave overtopping. It has a length overall of 90 m [60], its nominal power at 1:1 scale is expected to be 1.2 MW [61] and the transmission coefficient was obtained through laboratory tests [25]. Among the possible co-located layouts [8], a Peripherally Distributed Array (PDA), where WECs are placed on the perimeter of the wind farm as a barrier, emerges as the best option at the current stage of technology development [62]. The best results in terms of power production and shielding effect [63] were achieved for a layout with the co-located WECs protecting the farm not only from the predominant wave direction but also from the secondary directions. Moreover, previous studies on the interactions between devices[64] concluded that the best results were obtained considering the minimum allowed spacing between devices, $2.2L$, where $L$ = 90 m is the distance between the twin bows of a

single WaveCat WEC [65]. Due to the similarities of the proposed wind farm with Horns Rev wind farm, a ratio between the number of WECs and wind turbines of 0.7 was used, which led to optimum results in a recent study [35]. Thus, 56 WECs were deployed on a PDA layout oriented to the North to intercept the majority of incomings waves (Figure 4), with protection in particular against northwesterly waves since 315º was the predominant wave direction during the study period.

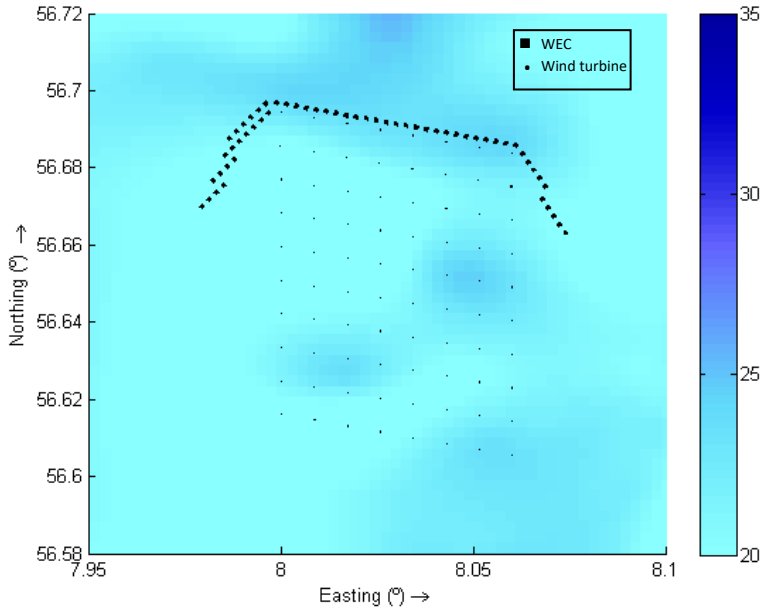


Figure 4. Co-located farm layout. The colour scale reflects the water depth in m.

## 3. Results and discussion

### 3.1. Wind and wave model validation

The results obtained from the two models used in this study (SWAN and WAsP) were successfully validated in terms of significant wave height and wind speed, respectively, with the metocean data from February 2005 to May 2015 provided by 3 buoys around the Horns Rev 3 wind farm. In both cases, a good correlation was observed between the simulated and measured time series (Figure 5). This was corroborated by the values of

the coefficient of determination ($R^2$), close to unity, and of the Root Main Square Error (*RMSE*) (Table 3).

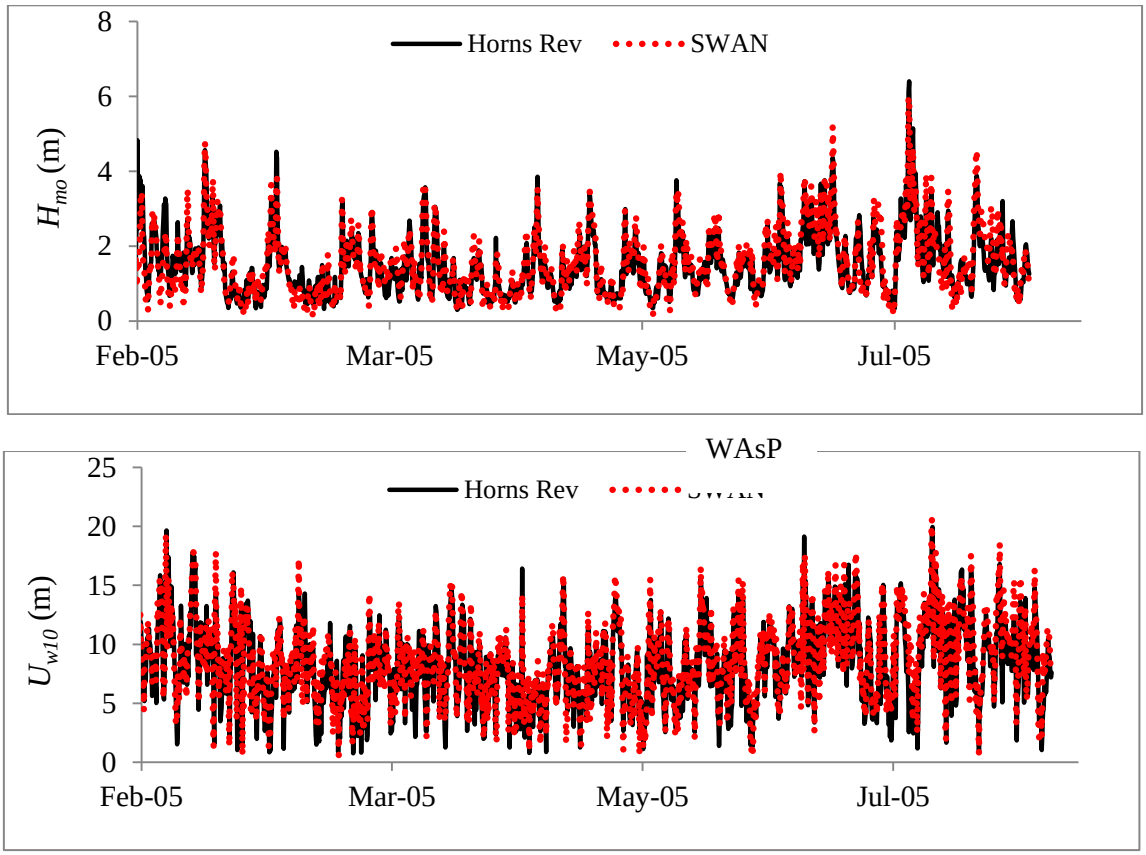


Figure 5. Correlation between hindcasts and metocean data from the buoy no.1 in the Horns Rev 3 area in terms of significant wave height ($H_{mo}$) and wind speed at 10 m above the sea level ($U_{10m}$) from February to August 2005.

Table 3. Coefficient of determination ($R^2$) and Root Main Square Error (*RMSE*) between hindcasts and measured significant wave height ($H_{m0}$) and wind speed at 10 m above the sea level ($U_{10m}$) from February 2005 to May 2013, for the three buoys considered.

| Buoy no. | $H_{m0}$ | | $U_{10m}$ | |
|---|---|---|---|---|
| | $R^2$ | *RMSE* (m) | $R^2$ | *RMSE* (m/s) |
| 1 | 0.93 | 0.41 | 0.87 | 0.20 |
| 2 | 0.93 | 0.38 | 0.86 | 0.21 |
| 3 | 0.90 | 0.34 | 0.87 | 0.27 |

### 3.2. Co-located farm results

The global energy production during the study period was approx. 1,500 GWh/year. The time-averaged power production of the wind turbines was around 160 MW, with a power output per wind turbine of approx. 2 MW, which implies a load factor – the real output of a turbine benchmarked against its theoretical maximum output in a year [66] – of 56%. The value is higher than the average, since this factor is commonly in the range of 35-45% [56, 67]. The wake losses (Figure 6) were 11.3%, similar or even lower than those observed in other wind farms currently in operation [68-70], which demonstrates the suitability of the proposed layout. When considering also the power production of the co-located WECs, the energy yield per unit of area increases by 3.4% with respect to the wind farm as a stand-alone installation. This implies a more sustainable use of the marine resource, a widely accepted goal for renewable resource management.

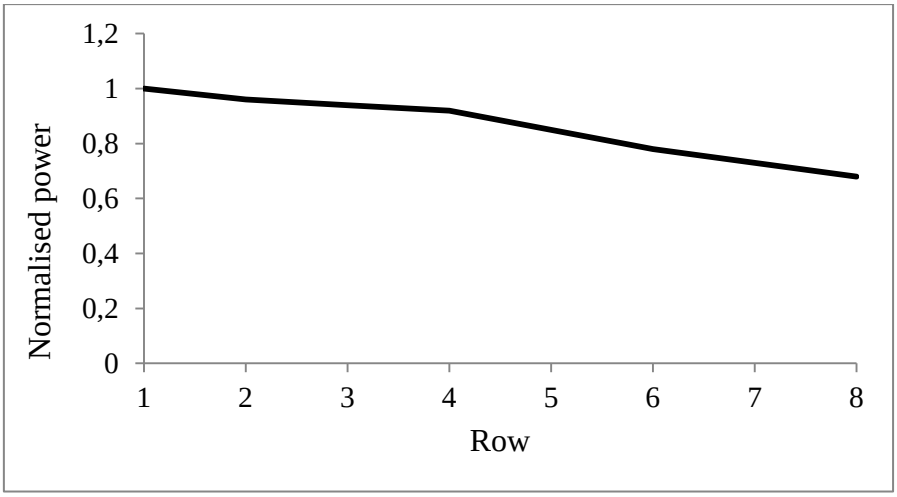


Figure 6. Evolution of the normalised power from the first row of wind turbines to the last as consequence of the wake effect.

Analysing the power output of the wind farm separately, its downtime was 6.6%, with most of it occurring during summer and spring due to the weaker winds. The combination with WECs decreased downtime to 2.74% − a significant reduction of

58.6%. Another benefit derived from combining wind and wave energy is the power smoothing that reduced the power variability and, consequently, the balancing cost when connecting the offshore installation to the grid. Comparing wave and wind farms as independent installations, it was found that the power generated by the wave farm presented larger inter – and intra- annual variability than in the case of the wind farm (Figure 7). In fact, the values of the *THD* during the study period for the wave and wind farm were 1.72 and 0.56, respectively. At first sight, it might appear that the aggregation of WECs to the wind turbines could increase the power output variability. However, the low correlation between both resources (Section 3.2) led to lower values of power variability for the co-located farm (*THD*: 0.49).

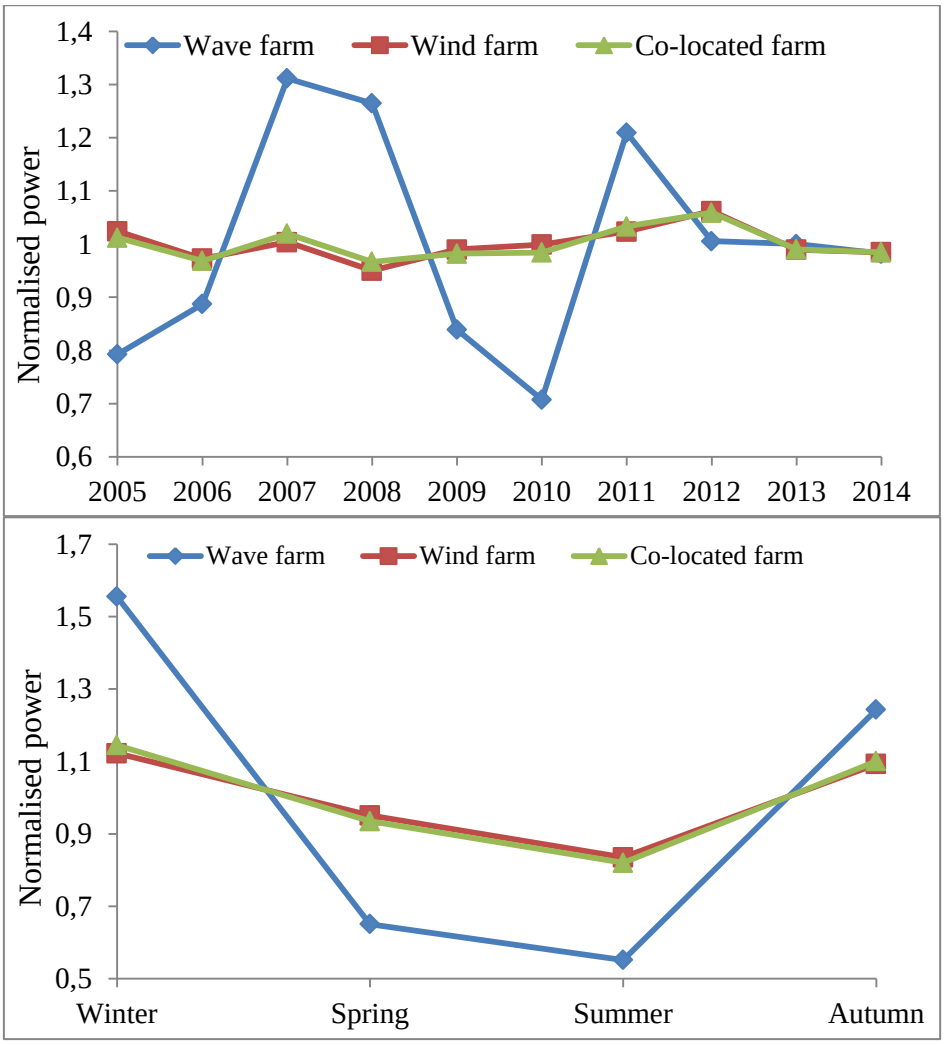


Figure 7. Inter- and intra-annual power output variability of the wave and wind farms as independent installations and the co-located farm.

The highest balancing cost due to power variability corresponds to the 15-minute variability. In this respect, the lag between waves and wind (Figure 8), with the highest cross-correlation factor for a lag of 1 hour, compensated the fluctuations to some extent and smoothed the power output. If wind speed is below the cut-in or above the cut-off values (the limits of production), wave energy could cover the power demand to some extent during this period.

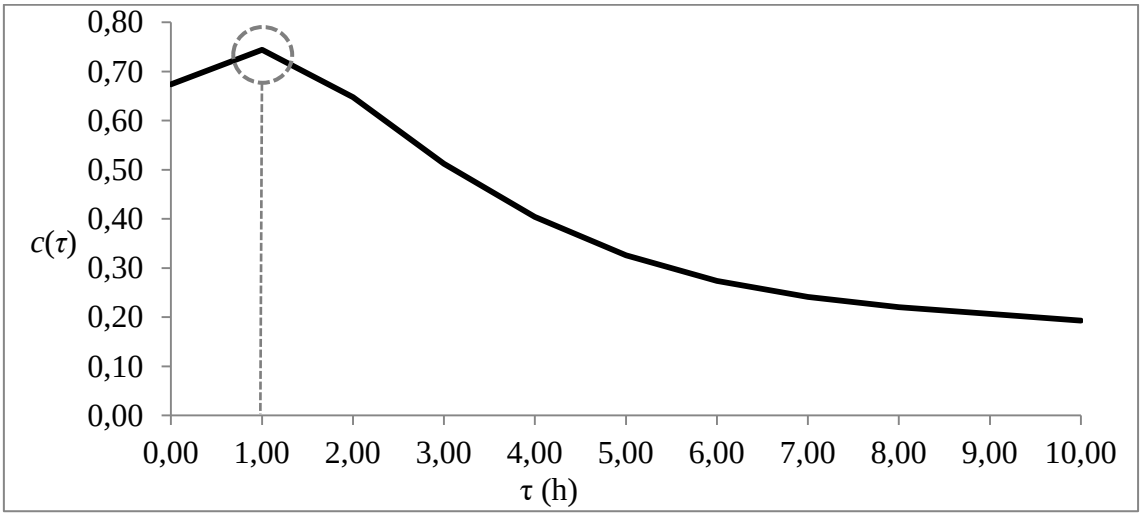


Figure 8. Correlation between wave and wind power at site no.7 for the study period; *c(τ)* is the cross-correlation factor and *τ* the time lag.

Apart from the benefits associated to the power production and its smoothing, the proposed combined system realises other synergies such as the shadow effect of the co-located WECs, which was evaluated in terms of the wave height reduction in the inner part of the wind farm. The global reduction (*HRF*) achieved was 7.93%. Its evolution with increasing distance from the barrier of WECs (*HRCj*) (Figure 8) showed a relatively uniform distribution of the wave height reduction, which decreased after the first row of with turbines due to the regeneration of waves with diffracted energy from the sides to increase again beyond the further rows thanks to the superposition of the individual shadow effects (wakes) of the different devices (Figure 9).

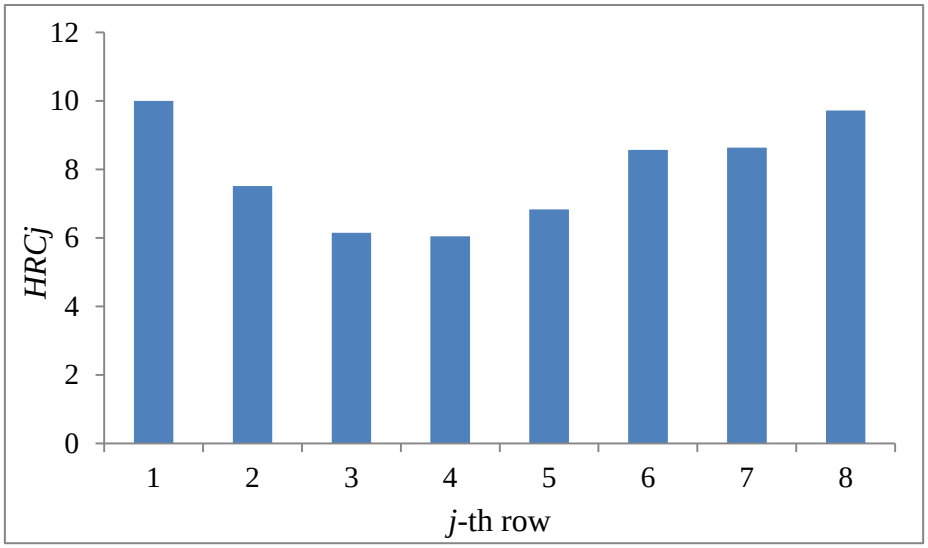

Figure 9. Evolution of the wave height reduction on each row of wind turbines as the distance from the WEC barrier increases.

The parameters above analysed – *HRF* and $HRC_j$ – were translated into accessibility terms. The operational limit to workboats is a significant wave height of 1.5 [71, 72]. In this case, the total number of hours when $H_s \leq 1.5$ m represented 57.39% of the year. Through the aggregation of the co-located WECs the accessibility increased to 68.45%, which involves an increase (*IA*) of nearly 20% (to be more precise, 19.27%). Remarkably, around 60% of the wind turbines experienced an increase in the accessible timeframe of approx. 10%, and 6% were accessible during 70-80% of the period considered (Table 4) – the latter being close to the co-located WECs.

Table 4. AWTk (%) values for the wind farm as an isolated installation and for the co-located farm .

| $k$ (%) | $AWT_k$ (%) | |
|---|---|---|
| | Wind farm | Co-located farm |
| = 100 | 0 | 0 |
| 90-100 | 0 | 0 |
| 80-90 | 0 | 0 |
| 70-80 | 0 | 6.25 |
| 60-70 | 0 | 61.25 |
| ≤60 | 100 | 32.5 |

The above benefits of the co-located farm in comparison with stand-alone wave and wind energy parks can be translated into monetary terms. The increase of the energy

yield per unit of area by 3.4% could reduce the site rental – which is around 3.3 €/MWh [73-75] – by a hefty 190,000 €/year. In the same line, the smoother power output would imply reductions in the balancing cost when connecting the offshore installation to the grid. This cost is estimated to range between 2.2 and 4.5 €/MWh for low wind power penetration levels [76]. In the case of the co-located farm analysed the output power variability was reduced by 12.5%. Following the methodology proposed in [77], the integration of wave and wind resources would involve a significant decrease of approx. 1 M€/year. For its part, increasing the accessibility to the wind turbines could avoid delays in unexpected repairs [78]. The estimated cost (or lost earnings) of delayed repairs is about 300 €/h [79, 80]. With this value as a reference, around 300,000 €/year would be saved thanks to the shadow effect of the co-located WECs. Moreover, the scheduled maintenance of the WECs and wind turbines carried out at the same time or one after the other reduces the cost associated with the transport of maintenance staff and the boarding of personnel onto the offshore structure. The same applies to labour cost, because this covers the cost of the O&M staff, which will typically be stationed on the project full time, and can be shared for both installations. Taking this into consideration, reductions of approx. 10% of the O&M cost can be achieved [81], which would correspond to savings of 4 M€/year for the co-located farm here analysed.

Moreover, combining different energy sources could reduce the capital cost by sharing common elements [5]. The cable for connection to the grid is more reliable and much cheaper if it is used to transport the maximum energy that it can carry. For this case, and applying the methodology proposed in [82], the cost of the export HVDC cable would be around 14 M€. Moreover, before exporting the electricity to shore the power has to be elevated from medium to high through a transformer. The cost of the offshore station would be around 3 M€. Therefore, if the cost of the electrical installation is

divided between both installations, the capital cost will be significantly reduced. Similarly, the cost of the preliminary studies, licenses and permissions would be reduced by 1 M€.

## 4. Conclusions

The aim of this paper was to assess the benefits of combining wave and wind energy systems relative to stand-alone farms through a case study in the Danish coast. The location for the proposed co-located farm (56.65ºN, 8.03ºE) was characterised by a distance to land of a mere 8 km, which would involve reduced installation and maintenance costs, water depths around 20 m, northwesterly predominant waves, westerly winds and 11.4 kW/m and 0.64 kW/$m^2$ as mean wave and wind power, respectively. The co-located farm proposed was composed by 80 turbines erected on a grid of 8 rows with monopiles as subtructures and a density of 5 MW/$km^2$. As for the co-located WECs, 56 floating, overtopping WECs were deployed as a barrier sheltering the farm from incoming waves to achieve a less energetic wave climate within the farm. The global energy production of the proposed farm during the study period was around 1,500 GWh/year, with a performance of the wind turbines around 56% (higher than the average) and wake losses of 11% (lower than the average) – which demonstrated the suitability of the proposed layout. The aggregation of the power output of the co-located WECs increased the energy yield per unit area by 3.4%, decreased downtime by 58% and reduced the power output variability by 12.5%. Moreover, the shadow effect of the co-located WECs within the wind farm increased the accessibility level by nearly 20%, with values close to 70% and with a fairly uniform distribution across the farm. All these benefits would involve cost savings around 1.5 M€/year in comparison to the wave and wind parks as stand-alone systems. Moreover, the capital cost and the maintenance costs would be reduced by 17 M€ and 4 M€/year, respectively, thanks to

the realisation of additional synergies, e.g. shared installations (submarine cable, transformer) and shared O&M staff. All in all, the reduced energy cost of co-located farms with regard to independent, stand-alone farms would enhance the competitiveness of ocean energy.

## Acknowledgments

This work was carried out in the framework of the Atlantic Power Cluster project (Atlantic Area Project nr. 2011-1/151, ATLANTICPOWER), funded by the Atlantic Area Operational Transnational Programme as part of the European Regional and Development Fund (ERDF). Astariz has been supported by the FPU grant 13/ 03821 of the Spanish Ministry of Education, Culture and Sport. The authors are grateful to the Horns Rev wind farm for the resource data of the site and to the European Marine Observation and Data Network (EMODnet) for the bathymetric data of the North Sea.

## References

[1] Atlas of UK Marine Renewable Energy Resources. Report No. R1106. Prepared for the UK Department of Trade and Industry, ABP Marine Environmental Research Ltd. (2004).
[2] BWEA. Marine Renewable Energy-State of the industry report. 2009.
[3] M. Veigas, G. Iglesias. Wave and offshore wind potential for the island of Tenerife. Energy Conversion and Management. 76 (2013) 738-45.
[4] S. Astariz, A. Vazquez, G. Iglesias. Evaluation of the levelised costs of tidal, wave and offshore wind energy. 3rd IAHR Europe Congress, Porto, Portugal, 2014.
[5] S. Astariz, G. Iglesias. Wave energy vs. Other energy sources: a reassessment of the economics. International Journal of Green Energy. In Press (2014).
[6] S. Astariz, G. Iglesias. Output power smoothing and reduced downtime period by combined wind and wave energy farms. Energy. 97 (2016) 69-81.
[7] S. Astariz, G. Iglesias. Enhancing Wave Energy Competitiveness through Co-Located Wind and Wave Energy Farms. A Review on the Shadow Effect. Energies. 8 (2015) 7344-66.
[8] C. Pérez-Collazo, D. Greaves, G. Iglesias. A review of combined wave and offshore wind energy. Renewable and Sustainable Energy Reviews. 42 (2015) 141-53.
[9] M.M.J. Carlos. Pérez-Collazo, Hannah. Buckland , Julia. Fernández-Chozas. Synergies for a wave-wind energy concept. EWEA, Vienna, 2013.
[10] S. Astariz, C. Perez-Collazo, J. Abanades, G. Iglesias. Co-located wind-wave farm synergies (Operation & Maintenance): A case study. Energy Conversion and Management. 91 (2015) 63-75.

[11] E.D. Stoutenburg, N. Jenkins, M.Z. Jacobson. Power output variations of co-located offshore wind turbines and wave energy converters in California. Renewable Energy. 35 (2010) 2781-91.
[12] S. Astariz, C. Perez-Collazo, J. Abanades, G. Iglesias. Towards the optimal design of a co-located wind-wave farm. Energy. 84 (2015) 15-24.
[13] N. Mortensen, D. Heathfield, O. Rathmann, M. Nielsen. Wind Atlas Analysis and Application Program: WAsP 11 Help Facility. Department of Wind Energy, Technical University of Denmark, Roskilde, Denmark 366 topics. (2014).
[14] I. Troen, E. Petersen. European Wind Atlas. Risø National Laboratory, Roskilde 656 pp ISBN 87-550-1482-8. (1989).
[15] H. Frank, O. Rathmann, N. Mortensen, L. Landberg. The Numerical Wind Atlas - the KAMM/WAsP Method. Roskilde, Denmark: Riso. (2001).
[16] O. Rathmann, R. Barthelmie, S. Frandsen. Turbine Wake Model for Wind Resource Software. European Wind Energy Conference and Exhibition. Denmark: Risoe National Laboratory. (2006).
[17] I. Katic, J. Højstrup, N. Jensen. A simple model for cluster efficiency. . European Wind Energy Association, Rome, 1986.
[18] R. Barthelmie, K. Hnsen, S. Frandsen, O. Rathmann, J. Schepers, W. Schlez, et al. Modelling and Measuring Flow and Wind Turbine Wakes in Large Wind Farms Offshore. Wind Energy. 12 (2009) 14.
[19] E. Miljødata. Case studies calculating wind farm production-Main Report. Denmark: Energi- og Miljødata. (2002).
[20] J. Abanades, D. Greaves, G. Iglesias. Coastal defence through wave farms. Coastal Engineering. 91 (2014) 299-307.
[21] A. Palha, L. Mendes, C.J. Fortes, A. Brito-Melo, A. Sarmento. The impact of wave energy farms in the shoreline wave climate: Portuguese pilot zone case study using Pelamis energy wave devices. Renewable Energy. 35 (2010) 62-77.
[22] N. Booij, Ris, R.C., Holthuijsen, L.H. A Third-Generation Wave Model for Coastal Regions 1.Model Description and Validation. J of Geophys Res. 104 (1999) 17.
[23] J. Abanades, D. Greaves, G. Iglesias. Wave farm impact on the beach profile: A case study. Coastal Engineering. 86 (2014) 36-44.
[24] T. Hayashi, Hattori, M., Kano, T., Shirai, M. Hydraulic Research on the Closely Spaced Pile Breakwater. Coastal Engineering. 50 (1966) 12.
[25] H. Fernandez, G. Iglesias, R. Carballo, A. Castro, J.A. Fraguela, F. Taveira-Pinto, et al. The new wave energy converter WaveCat: Concept and laboratory tests. Marine Structures. 29 (2012) 58-70.
[26] D.I. L. Freris. Renewable energy in power systems. John Wiley & Sons Inc (2008).
[27] D.W.I. Association. Available at: http://www.motiva.fi/myllarin_tuulivoima/windpower%20web/en/tour/wres/calculat.htm (Accessed on 20 July 2015).
[28] H.S.H.W.E. DEVELOPMENT. Environmental Impact Assessment - Noise & Vibration. Appendix 8.6 Wind Speed Calculations. Available at:

http://www.pfr.co.uk/documents/Appendix%208.6%20Wind%20Speed%20Calculations.pdf (Accessed on: 20 July 2015). (2010).
[29] R. Carballo, G. Iglesias. A methodology to determine the power performance of wave energy converters at a particular coastal location. Energy Conversion and Management. 61 (2012) 8-18.
[30] M.K. Ochi. Applied probability and stochastic processes. Wiley Inter-Science. (1990).
[31] J. Sjolte, G. Tjensvoll, M. Molinas. Power collection from wave energy farms. Applied Sciences. 3 (2013) 17.

[32] C. Beels, P. Troch, J.P. Kofoed, P. Frigaard, J. Vindahl Kringelum, P. Carsten Kromann, et al. A methodology for production and cost assessment of a farm of wave energy converters. Renewable Energy. 36 (2011) 3402-16.
[33] H. Lund. Large-scale integration of optimal combinations of PV, wind and wave power into the electricity supply. Renewable Energy. 31 (2006) 503-15.
[34] K. Daubney. Getting technicians to far-shore wind farms. in: W. OFFSHORE, (Ed.).2013.
[35] S. Astariz, J. Abanades, C. Perez-Collazo, G. Iglesias. Improving wind farm accessibility for operation & maintenance through a co-located wave farm: Influence of layout and wave climate. Energy Conversion and Management. 95 (2015) 229-41.
[36] S. Astariz, G. Iglesias. Accessibility for operation and maintenance tasks in co-located wind and wave energy farms with non-uniformly distributed arrays. Energy Conversion and Management. 106 (2015) 1219-29.
[37] J.P. Coelingh, A.J.M. van Wijk, A.A.M. Holtslag. Analysis of wind speed observations over the North Sea. Journal of Wind Engineering and Industrial Aerodynamics. 61 (1996) 51-69.
[38] U. Henfridsson, V. Neimane, K. Strand, R. Kapper, H. Bernhoff, O. Danielsson, et al. Wave energy potential in the Baltic Sea and the Danish part of the North Sea, with reflections on the Skagerrak. Renewable Energy. 32 (2007) 2069-84.
[39] K. Veum, L. Cameron, D.H. Hernando, M. korpås. Roadmap to the deployment of offshore wind energy in Central and Southern North Sea (2010-2030). WINDSPEED Suporting Decisions Supported by Intelligent Energy for Europe programme. (2010).
[40] 4COffshore. Horns Rev 1 Offhire Wind Farm. Available at: http://www.4coffshore.com/windfarms/horns-rev-1-denmark-dk03.html. 2016.
[41] Wind energy developments and Natura 2000. Guidance Document. in: E.C.I. 978-92-79-18647-9, (Ed.).2011.
[42] B. Saavedra-Moreno, S. Salcedo-Sanz, A. Paniagua-Tineo, L. Prieto, A. Portilla-Figueras. Seeding evolutionary algorithms with heuristics for optimal wind turbines positioning in wind farms. Renewable Energy. 36 (2011) 2838-44.
[43] S. Pookpunt, W. Ongsakul. Optimal placement of wind turbines within wind farm using binary particle swarm optimization with time-varying acceleration coefficients. Renewable Energy. 55 (2013) 266-76.
[44] A. Emami, P. Noghreh. New approach on optimization in placement of wind turbines within wind farm by genetic algorithms. Renewable Energy. 35 (2010) 1559-64.
[45] J.S. González, A.G. Gonzalez Rodriguez, J.C. Mora, J.R. Santos, M.B. Payan. Optimization of wind farm turbines layout using an evolutive algorithm. Renewable Energy. 35 (2010) 1671-81.
[46] X. Gao, H. Yang, L. Lu. Investigation into the optimal wind turbine layout patterns for a Hong Kong offshore wind farm. Energy. 73 (2014) 430-42.
[47] L. Chamorro, R. Arndt, F. Sotiropoulos. Turbulent flow properties around a staggered wind farm. Bound-lay Meteorol. 141 (2011) 349-67.
[48] F. Guillén. Development of a design tool for offshore wind farm layout optimization. Eindhoven University of Technology (2010).
[49] X. Gao, H. Yang, L. Lin, P. Koo. Wind turbine layout optimization using multi-population genetic algorithm and a case study in Hong Kong offshore. Journal of Wind Engineering and Industrial Aerodynamics. 139 (2015) 89-99.
[50] A. Crockford, P. Rooijmans, J. Coelingh, J. Grassin. Layout Optimisation for offshore Wind Farms. EWEA 2012: Europe`s Premier Wind Energy Event, Copenhagen, Denmark, 2012.
[51] O. Rahbari, M. Vafaeipour, F. Fazelpour, M. Feidt, M.A. Rosen. Towards realistic designs of wind farm layouts: Application of a novel placement selector approach. Energy Conversion and Management. 81 (2014) 242-54.
[52] R. Bansal, T. Bhatti, D. Kothari. On some of the design aspects of wind energy conversion systems. Energy Conversion and Management. 43 (2002) 2175-87.
[53] T. ATOW. Offshore wind technology overview. Albany, New York: Prepared for the Long Island-New York City Offshore Wind Collaborative by AWS Truewind, LLC (2009).

[54] M. Patel. Wind and power polar systems. CRC Press, Washington, DC. (1999).
[55] X. Sun, D. Huang, G. Wu. The current state of offshore wind energy technology development. Energy. 41 (2012) 298-312.
[56] Siemens. Thoroughly tested, utterly reliable. Siemens Wind Turbine SWT-3.6-120. Available at: http://www.energy.siemens.com/nl/pool/hq/power-generation/wind-power/E50001-W310-A169-X-4A00_WS_SWT_3-6_120_US.pdf (Accessed on 21 July 2015).
[57] N. Giese. REpower Offshore Wind Technology. Available at: http://mnre.gov.in/file-manager/UserFiles/presentations-offshore-wind-14082013/Norbert-Giese.pdf (Accessed on 21 July 2015). 2013.
[58] AREVA. Innovative Technology. Available at: http://www.areva.com/EN/operations-4430/areva-offshore-wind-innovative-technology.html (Accessed on 20 July 2015). (2013).
[59] J. Jonkman, S. Butterfield, W. Musial, G. Scott. Definition of a 5-MW Reference Wind Turbine for Offshore System Development. Technical Report NREL/TP-500-38060

Available at: http://homes.civil.aau.dk/rrp/BM/BM8/k.pdf (Accessed on 20 July 2015). (2009).
[60] G. Iglesias, H. Fernández, R. Carballo, A. Castro, F. Taveira-Pinto. The WaveCat© – Development of a new Wave Energy Converter World Renewable Energy Congress 2011, Linkoping, Sweden, 2011.
[61] A. Barrero. España apuesta por las olas. Energías Renovables, especial Energías del Mar. 106 (2011) 10.
[62] S. Astariz, C. Perez-Collazo, J. Abanades, G. Iglesias. Towards the optimal design of a co-located wind-wave farm. Energy. In Press (2015).
[63] S. Astariz, G. Iglesias. Co-located wave-wind farms: Economic assessment as a function of layout. Renewable Energy. In Press (2015).
[64] C. Perez-Collazo, S. Astariz, J. Abanades, D. Greaves, G. Iglesias. Co-located wave-wind farms: a preliminary approach to the shadow effect. International Conference on Ocean Energy (ICOE), Halifax, Canada, 2014.
[65] R. Carballo, G. Iglesias. Wave farm impact based on realistic wave-WEC interaction. Energy. 51 (2013) 216-29.
[66] D. Vicinanza, P. Contestabile, V. Ferrante. Wave energy potential in the north-west of Sardinia (Italy). Renewable Energy. 50 (2013) 506-21.
[67] A.B. WMJ Batten. An assessment of growth scenarios and implications for ocean energy industries in Europe. Sustainable Energy Research Group, School of Civil Engineering and the Environment, University of Southampton, Report for CA-OE, Project no 502701, WP5. (2006).
[68] R. Barthelmie, S. Frandsen, K. Hansen, J. Scepers, K. Rados, W. Sclez, et al. Modelling the impact of wakes on power output at Nysted and Horns Rev European Wind Energy Conference and Exhibition (EWEC), Marseille, France, 2009.
[69] G. Habenicht. OFFSHORE WAKE MODELLING Presentation at Renewable UK Offshore Wind 2011. Avalaible online at: http://www.res-group.com/media/17992/Offshore%20Wake%20Modelling%20-%20Presentation%20at%20Renewable%20UK%20Offshore%202011.pdf. (2011).
[70] R. Barthelmie. Wakes in large wind farms. Available online at: https://institutes.lanl.gov/ei/_docs/Annual_Workshops/Wind_Workshop_2011/Barthelmie_LosAlamos.pdf.
[71] G.G. Hassan. A Guide to UK Offshore Wind . Operations and Maintenance. Scttish Enterprise The Crown Estate. (2013).
[72] W.A.A.M.B.a.G.J.W.v. Bussel. The impact of different means of transport on the operation and maintenance strategy for offshore wind farms. Section Wind Energy, Faculty Civil Engineering and Geosciences, Delft University of Technology, The Netherlands (2002).
[73] D. Milborrow. Breaking down the cost of wind turbine maintenance. in: WINDPOWER, (Ed.).2010.

[74] M.I. Blanco. The economics of wind energy. Renewable and Sustainable Energy Reviews. 13 (2009) 1372-82.
[75] D.M. Alexander Lawrence. Offshore Wind Farm Operations & Maintenance. Benchmarks, Costs and best practices for current and future wind farms. . TA Cook. (2011).
[76] M.H. Albadi, E.F. El-Saadany. Overview of wind power intermittency impacts on power systems. Electric Power Systems Research. 80 (2010) 627-32.
[77] W. Katzenstein, J. Apt. The cost of wind power variability. Energy Policy. 51 (2012) 233-43.
[78] S. Enterprise. Innnovation in Offshore Wind. Installation, Operation & Maintenance.2012.
[79] L.W.M.M. Rademakers, H. Braam, T.S. Obdam, P. Frohböse, N. Kruse. Tools for estimating operation and maintenance costs of offshore wind farms: State of the Art. EWEC 2008, Brussels, 2008.
[80] I.D.a.D. McMillan. Sensitivity of Offshore Wind Turbine Operation & Maintenance Costs to Operational Parameters 42nd ESReDA Seminar Risk and Reliability for Wind Energy and other Renewable Sources Glasgow, UK, 2012.
[81] S. Astariz, C. Perez-Collazo, J. Abanades, G. Iglesias. Co-located wave-wind farms: Economic assessment as a function of layout. Renewable Energy. 83 (2015) 837-49.
[82] M. Dicorato, G. Forte, M. Pisani, M. Trovato. Guidelines for assessment of investment cost for offshore wind generation. Renewable Energy. 36 (2011) 2043-51.